Computer-Aided Design and Applications

http://www.cadanda.com

Simulating the Interaction between a Respirator and a Headform Using LS-DYNA

Jingzhou (James) Yang[1*], Jichang Dai[1] and Ziqing Zhuang[2]

[1]Texas Tech University, james.yang@ttu.edu, jichang.dai@ttu.edu
[2]National Institute for Occupational Safety and Health, zaz3@cdc.gov

ABSTRACT

Respirator use is an integral part of occupational safety and health practice. The challenge is to design respirators with the best fit and highest comfort level for all workers of diverse anthropometry. This paper presents a method to simulate the interaction between a respirator and a headform, and solutions for the universal design of respirators. Three-dimensional digital headforms and respirators are obtained using reverse engineering techniques. The commercial software, LS-DYNA, is used to model and simulate the interaction between a respirator and headform to determine the key factors that affect respirator fit and comfort. Both the respirator and headform are modeled as shell elements and are deformable. The results show that strap forces play an important role in pressure distribution on the face.

Keywords: respirator fit, headform, finite element analysis, stress and deformation.
DOI: 10.3722/cadaps.2009.539-551

1. INTRODUCTION

Respirators are devices designed to protect the wearer from inhalation of harmful dusts, fumes, vapors, or gases. Respirators come in a wide range of types and sizes and are used by the military, private industry, and the public. There are two main categories: the air-purifying respirator, which forces contaminated air through a filtering element, and the air-supplied respirator, in which an alternate supply of fresh air is delivered. The primary requirement for tight-fitting respirator design is to achieve a tight and comfortable fit to the user's face. The comfort assessment and respirator fit can be used for respirator design and certification testing in both civilian and military fields (Fig. 1). This study focuses on the first type of respirators.

Significant research has been done for air-purifying respirators used for military applications. One of the major directions is determining the relationship between the respirator seal pressure vs. fit factor and strap stretch. In the early work, protective respirators were evaluated directly by measurement of the fit factor (FF), a ratio of the concentration of particles outside versus the concentration of particles inside the respirator. Goldberg et al. [6,7] and Goldberg [5] measured pressure using air bladders constructed from heat-sealed sheets of plastic film sandwiched between sheets of cardboard to control expansion. The deflated bladder was placed beneath the mask-sealing surface and inflated until the cardboard sheets separated. The pressure at which separation occurred was interpreted as the seal pressure acting on the bladder. Jelier and Hughes [8] measured oronasal mask seal pressure using a Talley Oxford pressure-monitoring system. Lu [9] measured the pressure change in a pre-inflated air bladder placed between the M40 protective mask head harness pad and back of the head. Lu suggested that the head pad pressure was related to the seal pressure but did not prove that relationship. All of the previously used methods provided point measures of pressure that were difficult to interpret.

None of the previous researchers found a significant relationship between measured seal pressure and mask seal performance. Few researchers have attempted to measure seal pressure between a mask and face. Until recently, pressure sensors were ill-suited for measuring low pressures between two highly conformable surfaces such as the human face and rubber protective mask. In addition, the sensors that were available altered the fit of the mask when placed between the sealing surface and the face. Fit factor is an overall performance measure that does not provide any information about the location of leaks and therefore provides little feedback to the designer as to how to correct the problem. In addition, fit tests are expensive, time consuming, and cannot be performed on early prototype masks. Prototypes are commonly crude versions of the future mask and are usually not of the quality required to pass a chamber FF test. Thus, in the current mask design process, many important decisions are made before designers evaluate the most critical performance requirement, protection. Cohen [3] demonstrated that measuring and evaluating the pressure distribution between the mask sealing surface and face provides valuable information about seal integrity. Cohen also determined relationships between head harness strap stretch (a measure of strap tightness) and either FF or seal pressure.

Comfort is another important characteristic associated with respirators that many researchers have investigated ([4], [10-13], [17]).

Bitterman [2] investigated tools and procedures for rapid prototype development of environmental protection equipment for Air Force personnel. There are three components in Bitterman's work: computer interface program development; finite element modeling; and finite element analysis. Piccione et al. [13] developed the graphical and mathematical models of the M40 protective mask and the human face, and determined the interrelationship between the protective mask and face when the mask is worn. This study involved the use of a discomfort model, finite element analysis, laser scanning, and computer-aided design tools to perform the protective mask design task.

In our previous work [4], we carried out the feasibility study for the finite element analysis between a respirator and the human face using ANASYS software where the respirator was modeled as solid elements and the face as shell elements. Furthermore, the assumption was that the face is rigid. In this study, the advanced finite element software, LS-DYNA, is used for simulation due to its advanced contact solver. To save computation time, we model both the respirator and the headform as shell elements. The rigid face assumption is released to improve the fidelity of the model. Based on the deformable model, the results can be used to assess the respirator leakage and discomfort levels such as face tolerance, discomfort zone, sensitivity, tissue damage, and temperature on the face. Due to the deformable models, we can observe the dynamic contact process and pressure distribution.

This paper is organized as follows: Section 2 discusses the procedures for generating 3D digital models of respirators and headforms. Section 3 introduces the finite element modeling. Section 4 illustrates the finite element analysis. Finally, conclusions are given.

2. DIGITAL MODELS FOR HEADFORMS AND RESPIRATORS

In this section, we discuss the general procedures to develop the digital models of the headform and respirator (Zhuang and Viscusi, 2008). A Cyberware rapid 3D digitizer is the device used to record x, y and z coordinates of the human heads and respirators by scanning a large number of points on the object's surface and outputing a point-cloud data file. This data represents the visible surface of the object that has been scanned or digitized and can be processed later by CAD software.

2.1 Headforms

A total of 3,997 subjects was recruited by NIOSH in 2003 from industries and public services in which workers routinely or occasionally use respirators [19]. Among them, 1013 subjects (713 male and 300 female) were scanned by a Cyberware® 3D Rapid Digitizer. The criteria for choosing an individual 3-D head scan was based on calculations of principal components one (PC1) and two (PC2) [19]. Additional processing and measurement of the images was accomplished using Polyworks®. The headform dimensions for each size category were determined from the traditional data collected on all 3997 subjects surveyed. Every subject was placed into the Principal Component Analysis (PCA) fit test panel

using the algorithm in Zhuang and Viscusi (2008). Individuals with small heads fall into cell 1, medium heads in cells 2, 4, 5, and 7, large heads in cell 8, long heads in cell 6, and short heads in cell 3 (Fig. 2). Table 1 shows the measurements, in mm, of all subjects chosen for the averaging procedure. An algorithm was used to search through the 1013 scanned individuals to determine which subjects, in each size category, had dimensions closest to the mean values. For all scanned subjects, each of their 10 dimensions was first subtracted from the mean of each of the five head sizes. This difference was then divided by the standard deviation of each measurement for each size category, and then the squares of these values were added together. Subjects with the smallest sum were chosen to represent a given head size. Five face-size categories of PCA model were constructed by 10 facial dimensions relevant to respirator fit. For the ideal facial dimensions of each category, mean facial dimensions were computed. Finally, the representative headforms for each size were constructed from the average of five scans (Fig. 3).

Fig. 1: Respirator fit testing.

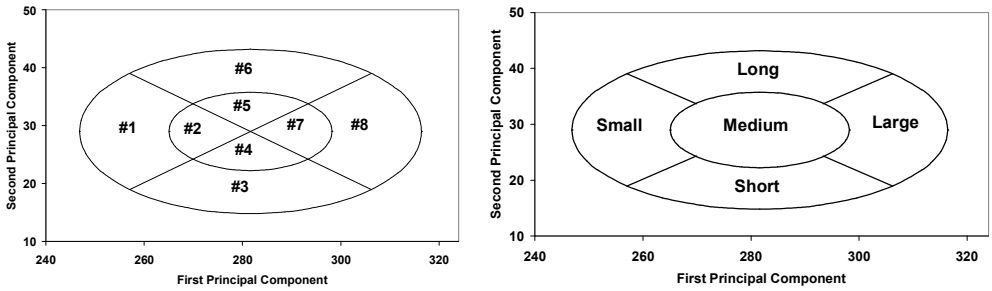

Fig. 2: Face size category on the PCA respirator fit test panel.

Designing a single headform is a multi-step process. Below is a description of the preliminary procedure used for the construction of the medium headform. After subjects were scanned, heads of the appropriate size and shape were selected, and their 3-D images were cleaned using Polyworks, a program that allows the user to edit 3-D scans. The first step was to properly align each head into a coordinate system from a determined symmetry plane and perpendicular to the Frankfurt plane (a plane passing through the inferior margin of the left orbit). Next, image spikes were eliminated, missing data was filled in, and hair on the top of the head and on the face was removed, resulting in a

watertight model. Fig. 4 shows one example of how the medium size headform is constructed. The final stage of the process was to average the 5 scanned heads together for the size category (small, medium, large, long and short), respectively, to create each digital 3-D headform.

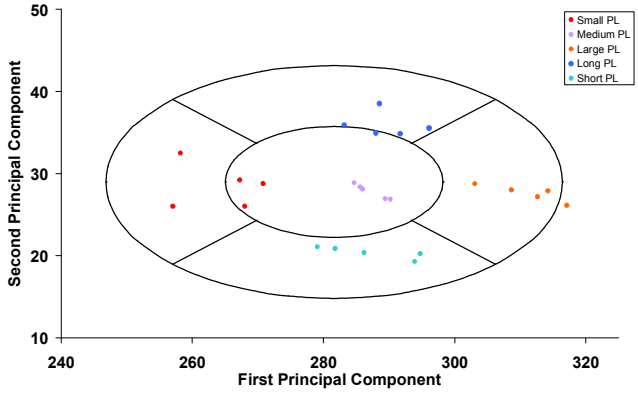

Fig. 3: Subjects selected for the creation of five headforms.

Including facial features that are not included in current design standards, five symmetric, digital 3D models were developed as shown from left to right in Fig. 5: small, medium, large, long/narrow and short/wide. These five headforms are supposed to be an adequate representation of the principal facial components of the U.S. worker population.

Size	Subject	Minimum Frontal Breadth	Face Width	Bigonial Breadth	Face Length	Inter-pupillary Distance	Head Breadth	Nose Protrusion	Nose breadth	Nasal Root Breadth	Subnasale-Sellion Length
	1	107	151	135	129	71	169	20	43	22	53
	2	115	150	149	126	67	169	22	40	21	54
Large	3	109	146	123	124	64	161	21	53	18	57
	4	114	162	137	133	65	160	20	38	20	50
	5	114	152	128	127	72	167	19	35	18	53
	1	106	137	122	118	61	161	18	29	20	51
	2	104	141	121	122	61	148	21	32	22	50
Medium	3	105	141	126	117	65	159	20	32	18	50
	4	98	146	126	117	60	163	16	38	16	51
	5	100	139	120	120	62	155	19	40	17	50
	1	91	135	106	112	56	153	17	33	17	50
	2	86	135	108	113	59	156	16	38	16	50
Small	3	93	128	92	108	58	150	16	31	18	46
	4	94	122	94	112	54	151	18	33	19	53
	5	101	131	100	110	63	154	16	29	18	49
	1	106	136	117	126	59	149	20	36	15	56
	2	96	134	125	130	63	157	18	37	17	55
Long	3	102	141	127	128	55	157	19	38	18	56
	4	96	145	128	129	58	162	22	42	18	55
	5	100	140	118	128	54	164	22	33	21	57
	1	99	142	115	114	64	163	17	40	22	45
	2	102	138	117	111	66	150	15	42	18	50
Short	3	108	150	132	111	59	159	18	41	17	46
	4	105	139	105	117	60	155	14	40	19	44
	5	107	151	122	108	64	167	17	41	17	49

Tab. 1: Polyworks measurements in mm of all subjects chosen for the averaging procedure.

2.2 Respirators

A MSA® brand Affinity Ultra respirator was scanned by the same 3D digitizer to form the point-cloud model, shown in Fig. 6. Fig. 6(a) shows the points that form the exterior appearance and also the holes. The point-cloud model contains an oxygen hose unnecessary for this research. The model also contains many missing planes and noisy points. It was first filtered by reverse engineering software to remove the noise and then sampled to reduce the roughness. After the point-cloud model was warped to a polygon model, these missing planes were repaired as shown in Fig. 7.

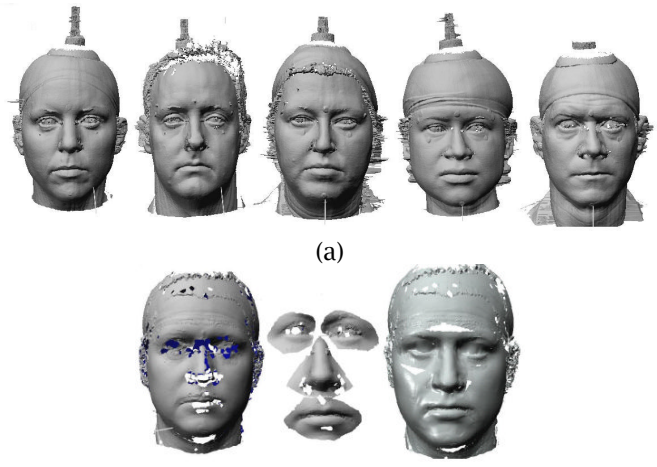

(a)

(b)

Fig. 4: The synthesis of the medium size headform: (a) the five subjects chosen for the medium headform along with the whole head average, the component averages; (b) the rough medium headform before smoothing and mirroring.

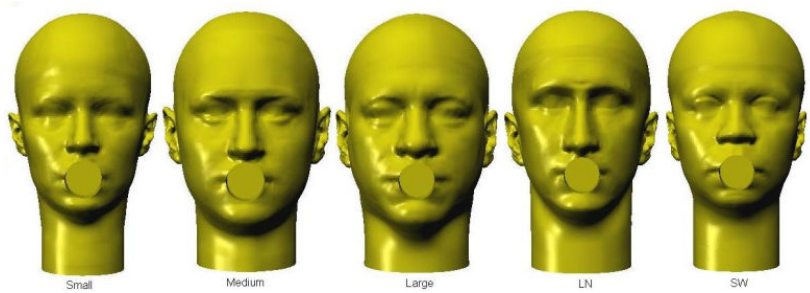

Fig. 5: NOISH Headforms in different sizes.

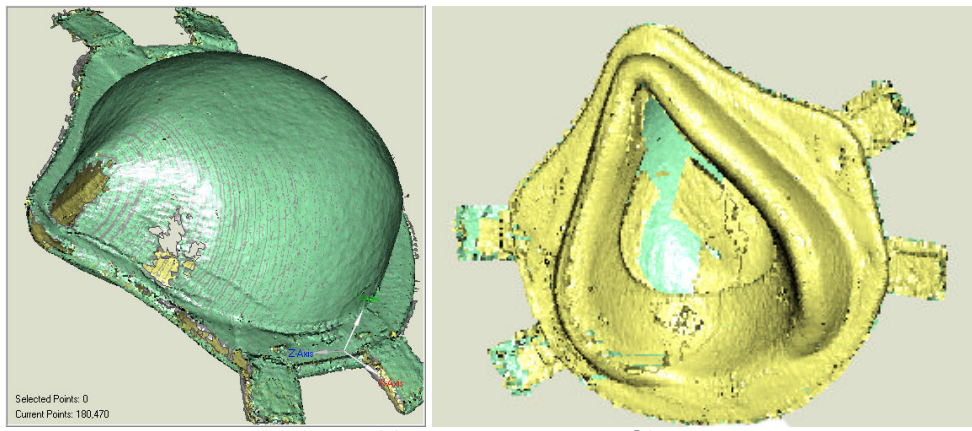

(a) (b)

Fig. 6: MSA® Affinity ultra respirator point-cloud model: (a) top and close view; (b) back and whole view.

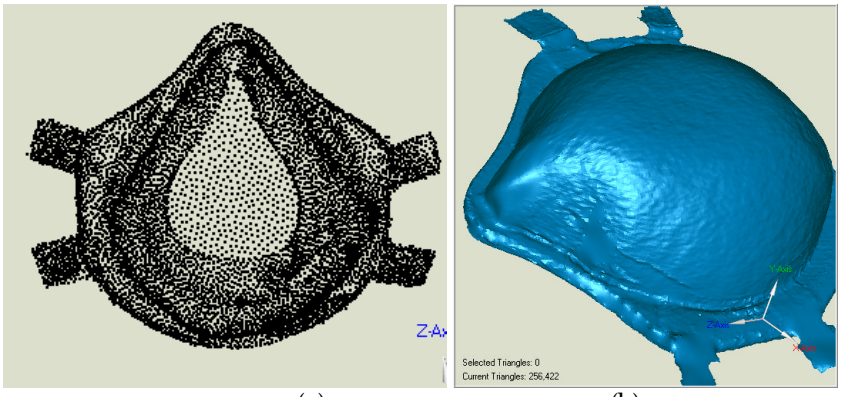

(a) (b)

Fig. 7: The processing results: (a) filtered and sampled model in points; (b) repaired polygon model.

To reduce the non-symmetry caused by the scanning and repairing process, only half of the polygon respirator model was further processed. A thickness of 2 mm was assigned to the polygon model before conversion of it to a CAD model (NURBS model). CAD software was employed to mirror the half-respirator and form the final model used for finite element analysis. Fig. 8 illustrates this procedure. We first generated the polygon model with thickness 0 mm in Fig. 8 (a), then, changed the thickness to 2 mm in Fig. 8 (b). Finally, we transformed the polygon model to CAD model.

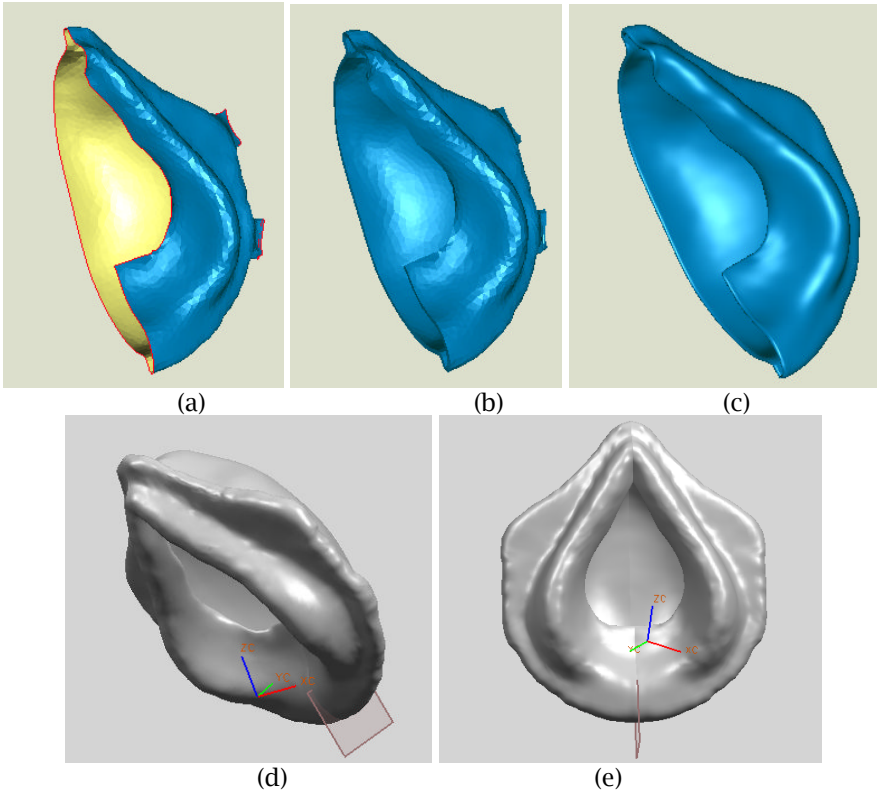

(a) (b) (c)

(d) (e)

Fig. 8: The procedure of transforming the polygon model to the CAD model: (a) thickness 0mm polygon model; (b) thickness 2mm polygon model; (c) half of the CAD model; (d) CAD model incline view; (e) CAD model back view.

To ensure accurate results, the digital respirator model must be as lifelike as possible. Comparison of the original point-cloud data model with the final CAD model shows only a deviation of less than 0.6mm, as seen in Fig. 9.

Finally, the respirator model and the large size headform model were assembled to form the respirator-headform pair shown in Fig. 10. This pair could then be imported into LS-DYNA for FEM modeling and analysis.

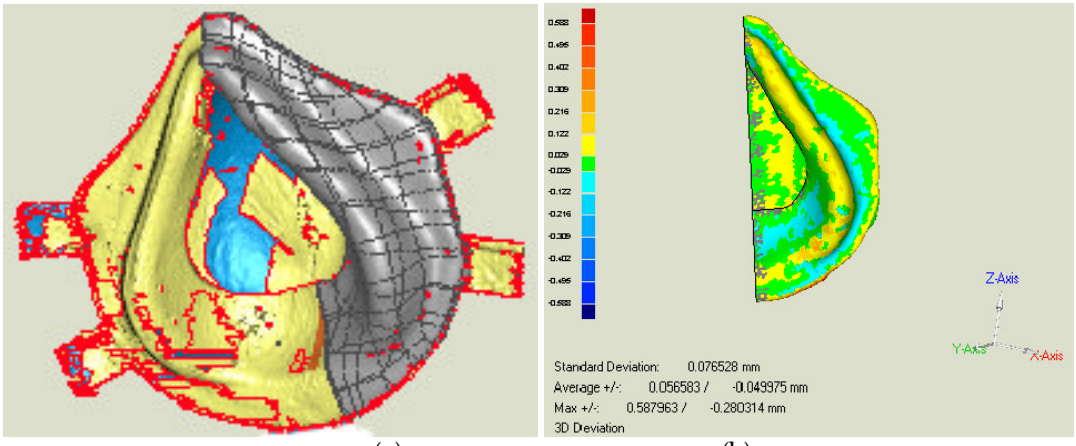

(a) (b)

Fig. 9: The checking procedure: (a) the superposition of CAD model and point-cloud model; (b) the deviation between the original point-cloud model and the constructed model.

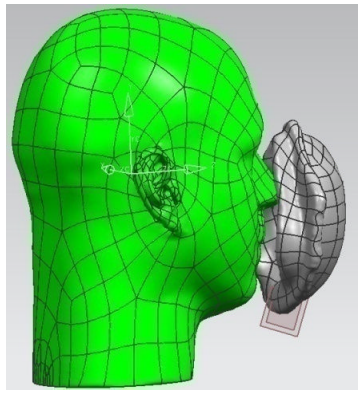

Fig. 10: The Respirator-headform pair.

3. FINITE ELEMENT MODELING

This section summarizes the finite element modeling. It includes model characteristics, model physical properties, material properties, and mesh generation.

3.1 Model Characteristics

To predict the registration of a respirator on a generic headform requires a finite element analysis tool capable of modeling large deformation along a complicated sliding contact surface. One such analysis tool is LS-DYNA. The LS-DYNA package has numerous material models and allows forces and boundary conditions to change during a simulation run. The ability to change the boundary conditions of a run can be very useful in the case of headform and respirator interaction. The respirator may be constrained to move along a specified path in the process of deforming to meet the shape of the headform. These constraints may then be replaced by others, which allow the deformed respirator to

hang on the headform, pulled downward by gravity, but still be constrained by the straps. The amount of contact between the respirator and the headform may then be quantified from the pressure induced on the surface elements of the headform by contact with the respirator elements. In this study, although we did not use these characteristics of LS-DYNA, in future study, we may further use these properties to improve the simulation results.

3.2 Respirator

Generally, respirators have several layers that are built from different materials. Affinity Ultra's respirator has an inner layer that is combined with the Silicone rubber sealing part, and an outer layer with a stiff cover designed to distribute the straps' loads. But in this simulation, only one layer of material was modeled. The material chosen is silicone rubber, which has an Elastic Modulus 2MPa. Silicone is a very deformable material with a Poisson's Ratio of nearly 0.5 (Bitterman, 1991). We use 0.499 instead of 0.5 to prevent the singularity of calculation. Although the density of silicone is about 0.87 g/cm^3, we use 1 g/cm^3 as the density to compensate for the assumption of one layer. The mesh was generated in the ANSYS/LS-DYNA environment and constructed with LS-DYNA shell163 element. The element shape is a quadrangle with an edge length of 5mm. The mesh is shown in Fig. 11.

3.3 Headform

The headform is modeled as a deformable shell model and the thickness of the shell element is 5 mm. Only the facial part of the whole headform is considered, because we are only interested in the interface between the respirator and face. A real human face is a complex combination of skin, muscles and bones. To construct a life-like face model is beyond the scope of this paper. We simplified the headform to only one layer and assumed it to have an Elastic Modulus of 2GPa with a Poisson's ration of 0.35, which are close to the mechanical properties of Nylon. The headform mesh generation is similar to the respirator and is shown in Fig. 12.

4. FINITE ELEMENT ANALYSIS

4.1 Load and Boundary Conditions

We used ANSYS/LS-DYNA as the pre-processor and solver to simulate the interaction process because of its capabilities in highly nonlinear dynamic finite element analysis with explicit time integration. We chose LS-PREPOST as the post-processor. Loads are applied on the four corners of the respirator where the straps are attached.

Because the front part of the head contacts with the respirator, the back part of the headform is constrained. Fig. 13 shows the meshed models along with the load and boundary conditions. The respirator is first moved to the contact status, then force is applied at four symmetrical points on the corner. There are no constraints on the respirator. The contact process between the respirator and headform happens when the respirator deforms. In this simulation, three different load values are applied on the straps. Strap loads are applied at the nodes associated with the ends of the straps. For the first case, each strap applies 2.5 N in the positive Z direction; for the second case, 5N on per strap; and for the third case, 7.5 N per strap. There are a total of four straps, and each strap load is applied on 50 nodes on the respirator shown in Fig. 13 (b).

4.2 Results

When the pre-process is completed, we run the solver and plot the results. We take snapshots of the respirator and headform from the contact process simulation at the initial contact, intermediate contact and final contact stage in Figs. 14-19. The initial contact stage is when the respirator and the headform contact. The intermediate contact stage is when the total number of contact points increase between the respirator and the headform. The final contact stage is when the straps are tightened.

The pressure (Figs. 14-16) on the sealing part of the respirator is unequally distributed, and the values are not significantly different for different strap tensions and contact stages. The maximum pressure for the 2.5 N case is 0.328 MPa, for the 5 N case is 0.062 MPa, and is 0.44 MPa for the 7.5 N case. All of the maximum pressures occur in the intermediate contact stage. There are two general insights: (1) For all load cases through the simulation process, the contact pressure first increases from the initial

contact stage to the intermediate contact stage, then decreases until the final contact stage; (2) with the strap force from 2.5 N, 5 N, to 7.5 N, the general tendency is that the maximum pressure first decreases, then increases. This pattern suggests that there is an optimal strap tension to achieve the minimum contact pressure with the highest comfort level.

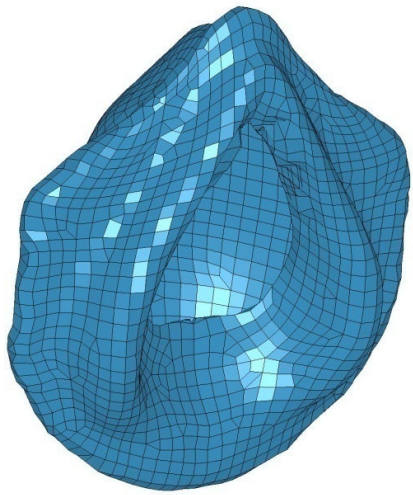

Fig. 11: The constructed mesh for the respirator.

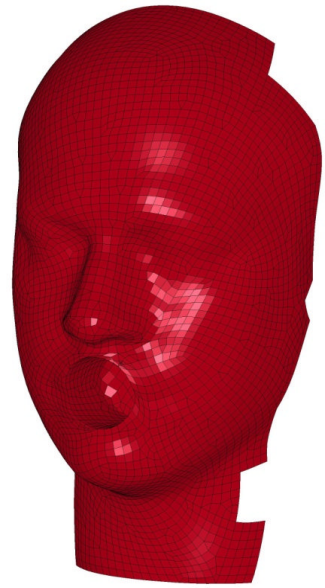

Fig. 12: The headform mesh.

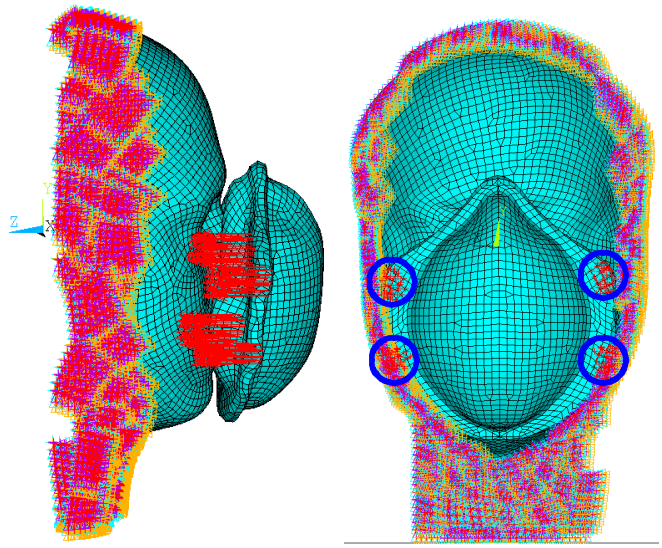

(a) Side view (b) Front view

Fig. 13: The external load and boundary conditions.

Within Figs. 17-19, we can draw a similar conclusion regarding the respirator. In addition, the highest pressure locations change with the interaction process. They occur around the nose bridge and cheeks. From Figs 17 to 19, the respirator is in contact with the face over the full circumference of the seal although the contact pressure at the bottom of the respirator is small.

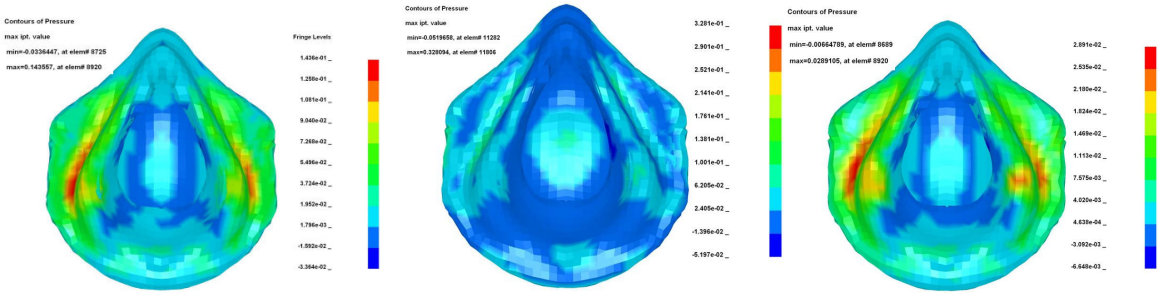

(a) (b) (c)

Fig.14: Respirator pressure with 2.5N tension on each strap. (a) Initial contact stage; (b) intermediate contact stage; (c) final contact stage

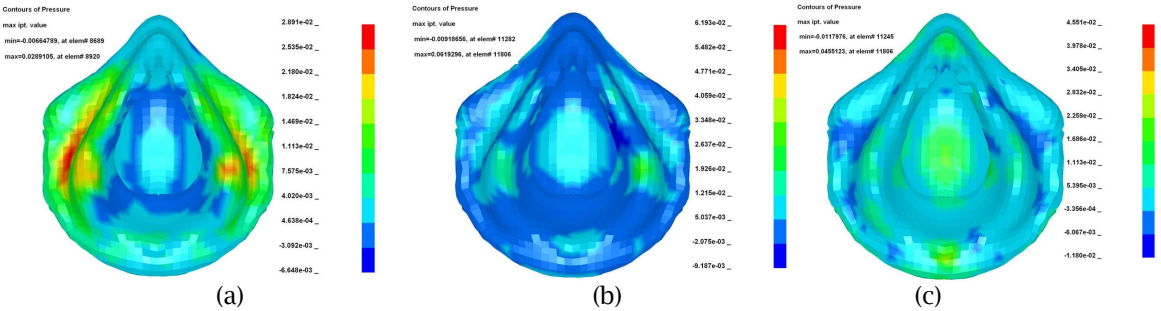

(a) (b) (c)

Fig.15: Respirator pressure with 5 N tension per strap. (a) Initial contact stage; (b) intermediate contact stage; (c) final contact stage

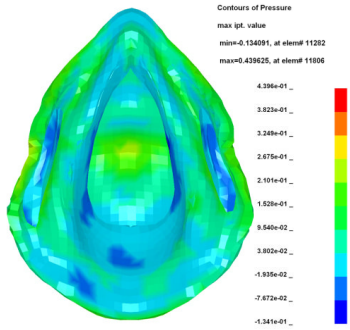

Fig.16: Respirator pressure of the intermediate contact stage with 7.5 N tension per strap.

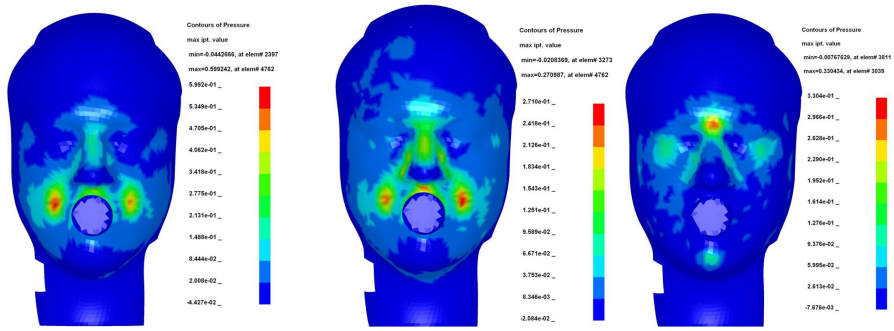

(a) (b) (c)

Fig. 17: The pressure distribution for the headform with 2.5 N tension per strap. (a) Initial contact stage; (b) intermediate contact stage; (c) final contact stage.

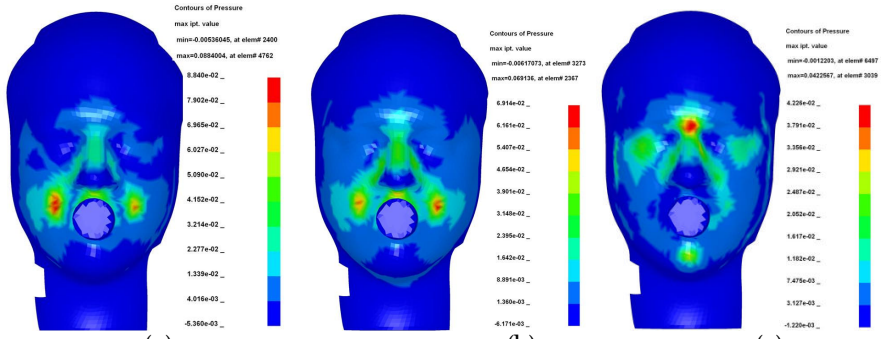

(a) (b) (c)

Fig. 18: The pressure distribution for the headform with 5 N tension per strap. (a) Initial contact stage; (b) intermediate contact stage; (c) final contact stage

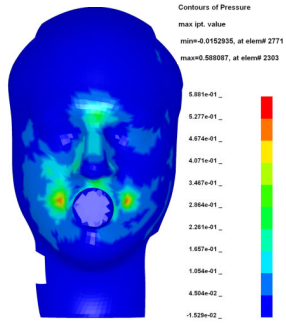

Fig. 19: The pressure distribution of the intermediate contact stage for the headform with 7.5 N tension per strap.

5. DISCUSSION

Current simulation has several limitations. The first limitation is the fidelity of the model. We use shell elements for both the respirator and headform. However, the respirator has several layers, and different layers are from different materials. The human face model has muscles, skin and bones. Therefore, both the respirator and the headform should be modeled as different layers. The second limitation is the materials. The material properties in this simulation are not accurate. The third limitation is the registration of the respirator to the headform. Currently we visually adjust the position between the respirator and the headform. The fourth limitation is that we have not investigated the effect of location of the respirator straps on the contact pressure.

6. CONCLUSION

A simulation model was developed for the interaction between a respirator and the headform using finite element software, LS-DYNA. The simulation model is based on the scanned 3D digital models of the respirators and headforms. In this study, we used the large respirator and large headform as one example. Different strap tensions were applied, and the whole interaction process was simulated from the initial contact stage to the final contact stage. The simulation shows that in all cases, the pressures on the headform and respirator are unevenly distributed. It also shows that with higher strap tension, the contact pressure decreases. However, with increasing strap tension, the contact pressure finally increases. The highest pressures occur on the areas of the nose bridge and cheeks. The contact pressure also changes throughout the interaction process (first increasing, then decreasing).

Future study includes the following goals:

- Improve the fidelity of the model for both the respirator and the headform.
- Investigate the effect of varying the location of the respirator straps on the contact pressure.
- Investigate the interaction between different types of headforms and different types of respirators.

- Develop a comfort model to virtually evaluate the respirator.
- Develop a fit model to virtually assess the respirator.

7. ACKNOWLEDGEMENTS
This research work is partly supported by the startup fund from Texas Tech University.

8. DISCLAIMER
The findings and conclusions in this work are those of the authors and do not necessarily represent the views of the National Institute for Occupational Safety and Health.

9. REFERENCES
[1] Akbar-Khanzadeh, F.; Bisesi, M.S.; Rivas, R.D.: Comfort of personal protective equipment, Applied Ergonomics, 26(3), 1995, 195-198.
[2] Bitterman, B. H.: Application of Finite Element Modeling and Analysis to the Design of Positive Pressure Oxygen Masks, Master Thesis, Air Force Institute of Technology, Wright-Patterson Air Force Base, OH, 1991.
[3] Cohen, K. S.: Relationship of Protective Mask Seal Pressure to Fit Factor and Head Harness Strap Stretch, Technical Report, Army Research Laboratory, Human Engineering and Research Directorate, Maryland, 1999.
[4] Dai, J; Yang, J.; Zhuang, Z.: Finite Element Analysis for the Interface of a Respirator and the Human Face-A Pilot Study, SAE Digital Human Modeling for Design and Engineering, June 9-11, 2009, Gothenburg, Sweden.
[5] Damascene, J.; Abeysekera, A.; Houshang, S.: Ergonomics aspects of personal protective equipment: its use in industrially developing countries, Journal of Human Ergology, 17, 1988, 67-79.
[6] Goldberg, M. N.: Individual respiratory protection against chemical and biological agents. Final report, Sections I and II, Unpublished manuscript, Edgewood Arsenal, MD: Defense Development and Engineering Laboratories, Physical Protection Laboratory, 1970.
[7] Goldberg, M. N.; Jones, R. E.; Wang, Y.; Crooks, T. P.: Individual respiratory protection against chemical and biological agents. Eleventh quarterly progress report (AD No. 8236533). Edgewood Arsenal, MD: Defense Development and Engineering Laboratories, Physical Protection Laboratory, 1967.
[8] Goldberg, M. N.; Raeke, J. W.; Jones, R. E.; Santschi, W. R.: Individual respiratory protection against chemical and biological agents. Sixth quarterly progress report (CB- 042964). Edgewood Arsenal, MD: Defense Development and Engineering Laboratories, Physical Protection Laboratory, 1966.
[9] Jelier, P.; Hughes, S.: Mechanical and anthropometric characteristics of soft tissue lavers in the head and maxillofacial region using combined mechanical and ultrasound techniques, Unpublished manuscript, University of Surrey, Guildford, UK, 1994.
[10] Lu, C.: Biomechanical comfort modeling of the M40 military gas mask. Unpublished manuscript. Aberdeen Proving Ground, MD: U.S. Army Research Laboratory, 1995.
[11] Manninen, A.; Klen, T.; Pasanen, P.: Evaluation of Comfort and Seal Leakages of Several Respirators Used in Agricultural Work, American Industrial Hygiene Association Journal, 49(6), 1988, 280-285.
[12] Mols, G.; Von Ungern-Sternberg, B. C.; Rohr, E. C.; Haberthur, C.; Geiger, K.; Guttmann, J.: Respiratory comfort and breathing pattern during volume proportional assist ventilation and pressure support ventilation: A study on volunteers with artificially reduced compliance, Critical Care Medicine. 28(6), 2000, 1940-1946.
[13] Piccione, D.; Moyer Jr, E. T.; Cohen, K. S.: Modeling the Interface between a Respirator and the Human Face, Technical Report, Army Research Laboratory, Human Engineering and Research Directorate, Maryland, 1997.
[14] Shimozaki, S.; Harber, P.; Barrett, T.; Loisides, P.: Subjective tolerance of respirator loads and its relationship to physiological effects, Am. Ind. Hyg. Assoc. J. 49(3), 1988, 108-116.
[15] Snook, S. H.; Hinds, W. C.; Burgess, W. M. A.: Respirator Comfort: Subjective Response to Force Applied to the Face, American Industrial Hygiene Association Journal, 27(2), 1966, 93-97.

[16] Weiss, R. A.; Pasternak-Silva, J.: Physiological Evaluation of First Responder Mask, Army Research Laboratory, Human Engineering and Research Directorate, Maryland, 2003.
[17] White, M. K.: Work tolerance and subjective responses to wearing protective clothing and respirators during physical work, Ergonomics, 32(9), 1989, 1111-1123.
[18] Zhuang, Z.; Bradtmiller, B.: Head and face anthropometric survey of U.S. respirator users, J. Occup. Environ. Hyg., 2, 2005, 567-576.
[19] Zhuang, Z.; Bradtmiller, B.; Shaffer, R.: New Respirator Fit Test panels representing the current U.S. Civilian Work Force, J. Occup. Environ. Hyg., 4, 2007, 647-659.
[20] Zhuang, Z.; Viscusi, D.: A new approach to developing digital 3-D headforms, SAE Digital Human Modeling for Engineering and Design, June 14-17, 2008, Pittsburgh, PA.